



Optical and structural investigation of In_{1-x}Ga_xP free-standing microrods

M. K. K. Nakaema, M. P. F. Godoy, M. J. S. P. Brasil, F. Iikawa, D. Silva, M. Sacilotti, J. Decobert, and G. Patriarche

Citation: *Journal of Applied Physics* **98**, 053506 (2005); doi: 10.1063/1.2033150

View online: <http://dx.doi.org/10.1063/1.2033150>

View Table of Contents: <http://scitation.aip.org/content/aip/journal/jap/98/5?ver=pdfcov>

Published by the [AIP Publishing](http://www.aip.org)

Articles you may be interested in

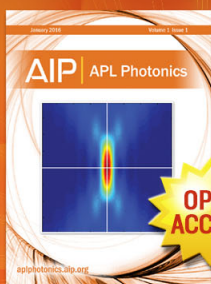
[Spontaneous formation of InGaN nanowall network directly on Si](#)
Appl. Phys. Lett. **102**, 173105 (2013); 10.1063/1.4803017

[Heteroepitaxial growth of GaN/Si \(111\) junctions in ammonia-free atmosphere: Charge transport, optoelectronic, and photovoltaic properties](#)
J. Appl. Phys. **113**, 124304 (2013); 10.1063/1.4798266

[Free-standing, optically pumped, GaN/InGaN microdisk lasers fabricated by photoelectrochemical etching](#)
Appl. Phys. Lett. **85**, 5179 (2004); 10.1063/1.1829167

[Influence of strain relaxation on structural and optical characteristics of InGaN/GaN multiple quantum wells with high indium composition](#)
J. Appl. Phys. **91**, 1166 (2002); 10.1063/1.1429765

[Fabrication and photoluminescence of ordered GaN nanowire arrays](#)
J. Chem. Phys. **115**, 5714 (2001); 10.1063/1.1407005



Launching in 2016!
The future of applied photonics research is here

AIP | APL
Photonics

Optical and structural investigation of $\text{In}_{1-x}\text{Ga}_x\text{P}$ free-standing microrods

M. K. K. Nakaema,^{a)} M. P. F. Godoy, M. J. S. P. Brasil, and F. Iikawa^{b)}
*Instituto de Física "Gleb Wataghin," Universidade Estadual de Campinas (UNICAMP), Caixa Postal 6165,
 Campinas-São Paulo (SP), CEP 13083-970, Brazil*

D. Silva
*Instituto de Geociências, Universidade Estadual de Campinas (UNICAMP), Caixa Postal 6152, Campinas-
 São Paulo (SP), CEP 13083-970, Brazil*

M. Sacilotti
*Couches Minces et Nanostructures Group, FR 2604 Centre National de la Recherche Scientifique (CNRS),
 Université de Bourgogne, 21078 Dijon, France*

J. Decobert
Alcatel-CIT, Route de Nozay, 91460 Marcoussis, France

G. Patriarche
*Laboratoire de Photonique et de Nanostructures, Centre National de la Recherche Scientifique (CNRS),
 Route de Nozay, 91460 Marcoussis, France*

(Received 22 December 2004; accepted 18 July 2005; published online 2 September 2005)

We present a structural and optical characterization of scepterlike micrometer-sized free-standing structures, composed of a long InGaP rod with a metallic sphere on its top, grown on polycrystalline InP substrates. In contrast to the conventional vapor-liquid-solid growth method, no catalyst was deposited on the substrate. Instead, metallic In liberated from the InP substrate by phosphor evaporation works as the catalyst metal. We performed Raman scattering, photoluminescence spectroscopy, scanning electron microscopy, and energy dispersive x-ray spectroscopy measurements on individual structures. The alloy composition measured by microscopic techniques is in agreement with the values obtained by the optical measurements considering that the rod is strain free. The InGaP rods present essentially constant Ga composition within a fluctuation of $\sim 10\%$ and efficient optical emission. We also observed a marked increase in the Raman-scattering signal at rod positions near the metallic sphere (the "neck"), which was attributed to a surface-enhanced Raman-scattering effect. Our results demonstrate the possibility of using InGaP rods for optical device applications. © 2005 American Institute of Physics.

[DOI: [10.1063/1.2033150](https://doi.org/10.1063/1.2033150)]

I. INTRODUCTION

Recently, free-standing nano- and microsized wires, also known as rods or whiskers, have been explored,^{1–8} due to their potential applications in electronic and photonic devices. Free-standing nano- microwires have been synthesized via various different methods, including hot carbon plasmas, vapor-phase evaporation, laser ablation, template-based techniques, and catalytic reactions.⁷ A broad goal of the area is to obtain nano-objects with controlled sizes and shapes, which may be used to investigate phenomena related to quantum effects.⁸ Catalytic synthesis based on the vapor-liquid-solid (VLS) growth mechanism is a promising candidate for this purpose.^{8,9} This method has been widely used to produce several kinds of nano-objects, including binary¹⁰ and ternary⁷ metal oxides and III-V semiconductor nanowires.^{1,2,4,11,12} The growth mechanism is based on using metallic nanocluster catalysts, which become liquid nanodrops at the growth temperature and, mixed with the growth elements, start the growth in a strongly anisotropic way generating long wire-like structures.⁹

We investigated InGaP free-standing microrods grown on polycrystalline InP substrates by an alternative VLS-like method using a low-pressure metal-organic chemical-vapor deposition (MOCVD) reactor. This technique was recently demonstrated by Sacilotti *et al.*,¹³ as a method to grow free-standing microrods. In contrast with the conventional VLS growth mechanism, no metal catalyst was deposited on the substrate. Instead, metallic In, liberated from the InP substrate by phosphor evaporation, works as the catalyst metal. The absence of the additional catalyst metal reduces the incorporation of impurities and defects.¹⁰ We believe, however, that the growth mechanism of this method is similar to that of the VLS method, since both result in the formation of free-standing rods with metallic particles (spheres) at their tops. In our case, the metallic spheres are formed mainly of In and Ga coming from the substrate during the growth and from the metal-organic precursor. The growth of nanorods without metal catalysts has been presented before for ZnO rods on Al_2O_3 substrates.¹⁰ In that case, however, the growth was not induced by a metallic drop formed from the substrate as occurs in our system, but from ZnO nucleation points formed at the substrate.

We present here the results of Raman scattering, photo-

^{a)}Electronic mail: mnakaema@ifc.unicamp.br

^{b)}Electronic mail: iikawa@ifc.unicamp.br

luminescence, scanning electron microscopy (SEM), and energy dispersive x-ray (EDX) measurements of free-standing InGaP rods. The analysis of our data is useful for understanding the growth dynamics of these structures. We observed that the InGaP microrods show good crystalline and optical qualities and reasonable homogeneity along the rod for lengths as long as $10\ \mu\text{m}$. This result is a good indication that these materials can be used for technological applications. The large band gap of the InGaP alloy (up to 2.2 eV for direct band-gap material) makes it very interesting for applications on visible-light-emitting devices. Furthermore, the growth of micro- and nanorods of semiconductor ternary alloys brings out a desirable versatility of several of the micro- and nano-object properties, which could be efficiently tuned by adjusting the composition ratio.

II. EXPERIMENTAL DETAILS

The InGaP structures were grown on polycrystalline InP substrates by the MOCVD technique using N_2 as the carrier gas [5–10 standard liter per minute (SLM)] and a reactor pressure from 760 to 100 torr. Millimeter-sized grain InP polycrystal substrates were used, after polishing them with a Br-methanol standard technique. During growth, the sample was subjected to a flux of trimethyl gallium (TMGa), as the gallium source. The TMGa organometallic flux was maintained as the only gas source for typically 5–15 min, while neither additional group III, nor group V elements, arrived at the sample surface. We present the results of two distinct samples grown at different temperatures: sample A ($700\ ^\circ\text{C}$) and sample B ($650\ ^\circ\text{C}$).

Raman-scattering measurements were performed at room temperature in the backscattering geometry using the 488-nm line of an Ar-ion laser with intensities of the order of $\sim 0.5\ \text{mW}$ focused in a diameter spot size of $\sim 1\ \mu\text{m}$. The scattered light was analyzed using a T64000 Jobin-Yvon Raman system with a triple spectrometer and a liquid-nitrogen (LN_2)-cooled charge-coupled device (CCD). The linear polarization of the laser beam was kept parallel to the rod length and the scattered light was integrated without polarization analysis. Microphotoluminescence (micro-PL) measurements were performed at $\sim 10\ \text{K}$ using a cold-finger He cryostat; for photoexcitation we have used the 488-nm line of an Ar-ion laser focalized through a large working distance with $50\times$ objective and the luminescence was detected using a 0.5-m monochromator coupled to a GaAs photomultiplier. The SEM was performed using a LEO 430i system from Zeiss coupled to a CatB EDX from Oxford Microanalysis Group. We used a 20-kV accelerating voltage and a 6-nA probe current in backscattering mode, with the microrods directly fixed in a carbon conductive tape. For quantitative analysis we have used a ZAF correction program with pre-recorded standards.

III. RESULTS

The TMGa interaction with the poly-InP substrate surface gives rise to free-standing InGaP rods, with a sphere at the top of each, resulting in a scepterlike shape, as shown by the SEM picture in Fig. 1. The rod diameters are of the order

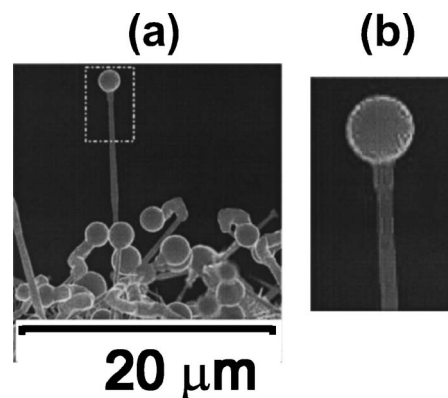


FIG. 1. (a) SEM picture of InGaP scepterlike structures from sample A and (b) an enlarged view of the selected region in (a); Note the “neck” close to rod/sphere interface.

of $0.1\text{--}0.5\ \mu\text{m}$ and their lengths vary from a few microns up to a few tens of microns. The structures at the top are nearly spherical and their diameters vary from 0.1 up to $3\ \mu\text{m}$. Previous microscopic elemental analysis¹³ showed that each sphere is mostly composed of In and the rods are composed of an InGaP single crystal capped by a thin layer of amorphous Ga oxide that is likely formed when the sample is exposed to air after growth.^{14,15} The angle of the rod axis relative to the substrate surface is rather random since it depends on the orientation of the poly-InP grain from which each rod originates. Transmission electron microscopy (TEM) results indicate that the rod axes grow mostly along the $\langle 111 \rangle$ and $\langle 113 \rangle$ directions.¹³ For optical measurements, we always selected isolated rods in order to avoid mixed signals.

Figure 2 shows typical Raman spectra from one InGaP rod. The Raman spectra were obtained at various points along a single rod from sample A. The points correspond to uniformly spaced positions along the rod length, considering the metallic sphere as the “top” and the point where the rod is connected to the substrate as the “bottom.” They present three typical features usually observed in InGaP bulk alloys: a TO band, a LO band, and an intermediate feature denoted here by I.^{16,17} A controversy still persists as to the vibrational mode behavior of InGaP. Beserman *et al.*¹⁸ interpreted their results on the basis of one-mode behavior. In contrast, Abdelouhab *et al.*¹⁹ proposed a two-mode behavior for strained,

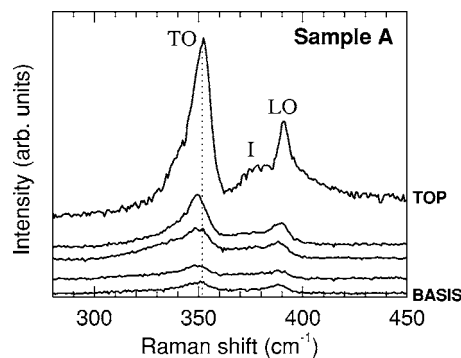


FIG. 2. Raman spectra of a typical rod from sample A. Three features could be assigned to TO, LO, and the intermediate feature I, respectively.

InGaP heterostructures, and Jusserand and Slempek²⁰ proposed a “modified” two-mode behavior for InGaP samples. In the one-mode picture, I is associated with a disorder-activated mode, whereas in the two-mode picture the TO and LO peaks are assigned to GaP-like modes and the additional feature is interpreted as a LO InP-like mode. On the other hand, in GaP nanorods, a similar I was associated with a surface optical-phonon mode activated by periodic oscillations in the wire cross section along its length.² Most of these authors observed, however, that the TO peak position varies in an approximate linear way with the InGaP alloy composition. Therefore, we may use the TO phonon position as a probe of the InGaP rod composition.

A remarkable effect concerning the Raman signal intensity is clearly evident in Fig. 2: the Raman signal is significantly stronger at the top of the rod (close to the metallic sphere) as compared with the remainder of the rod length. This effect was observed for some rods with an enhancement factor varying from 10 to as large as 100. There is no evidence of a crystal quality improvement at such points that could explain such enhancements. For instance, the linewidth of the Raman peaks remains basically constant, showing no narrowing at those points. The complexity of the measurement, and therefore the limited number of points, results in relatively restricted statistics. We observed, however, that this enhancement effect has some correlation with the shape of the capping oxide layer. An unambiguous and conclusive observation is that the Raman intensity enhancement only occurs at rod positions very close to the metallic sphere (top), in regions where the capping layer of the rod is relatively thick and inhomogeneous, forming a sort of “neck” connecting the rod to the sphere [Fig. 1(b)]. We thus suggest that the signal improvement may be related to a surface-enhanced Raman-scattering effect (SERS).^{21,22} It is well known that the enhancement factor related to SERS depends on the metal surface: domain size, roughness, and other factors^{21,22} and an optimum situation may occur only close to the neck of the rod. This phenomenon, however, should be investigated in more detail.

The Ga composition of various InGaP rods from samples A and B was investigated using Raman-scattering measurements. The alloy composition along the rod length was estimated from the TO peak position, as discussed above. We calculated the alloy composition using a linear dependence of the TO phonon peak, the frequency of which goes from 303.7 cm^{-1} in pure InP to 367.0 cm^{-1} in pure GaP.²³ In our analysis we considered the rods as being free from strain. Figure 3 shows the Ga content for various rods from both samples A and B as a function of rod length. In sample B the measured rods had lost their spheres, so that it was not possible to tell top from bottom. We measured, however, a large number of pristine scepterlike rods from sample A. Figure 3(a) shows the results of three representative scepterlike rods from sample A. The origin of the x axis corresponds to the top of the rods. The Ga concentration for all measured rods from sample A is within 0.70 ± 0.15 . We did not observe any systematic correlation between the Ga concentration and the relative position along the rod. Even though some rods show a strong Ga variation along their length (up to $\Delta x \sim 0.3$), we

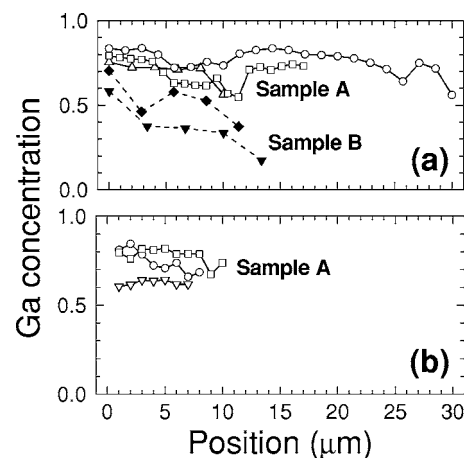


FIG. 3. (a) Ga content of the InGaP rods of samples A (open symbols) and B (filled symbols) determined by Raman scattering and (b) the Ga content of the rods of sample A determined by EDX analysis.

measured several rods with relatively extended regions (up to $\sim 10 \mu\text{m}$) where the Ga composition remains reasonably constant within less than 0.05. This composition homogeneity is an important positive factor for device applications. The Ga composition was also estimated by EDX measurements for various rods from sample A. The results are presented in Fig. 3(b) as a function of the rod length and are in good agreement with the composition estimated by the Raman spectra. We also present the estimated Ga composition for two distinct rods from sample B [Fig. 3(a)] using Raman spectroscopy. In this case, the average Ga composition is ~ 0.50 and the measured rods show a relatively large composition variation as compared with sample A. The Ga composition of one rod from sample B was previously measured by TEM,¹³ giving a Ga composition of 0.47–0.49, which is also in agreement with the composition we had estimated by Raman measurements. TEM results are very precise since they are based on the directly measured lattice constant of the structure. However, TEM is neither an appropriate technique to determine the statistics of various distinct rods nor to evaluate the composition along a rod length, since it involves complex measurements and it is usually restricted to a small number of pictures.

We have also performed Raman measurements from the

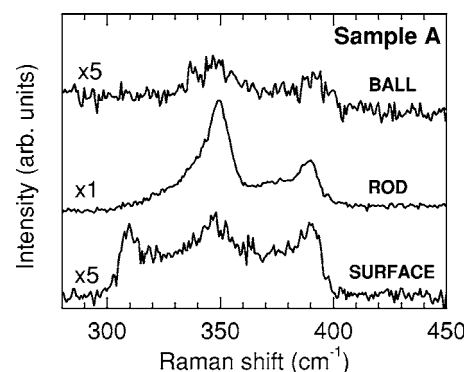


FIG. 4. Raman spectra of a sphere, the substrate surface, and a rod from sample A. The Raman signal from the sphere and substrate surface is much smaller than the rods.

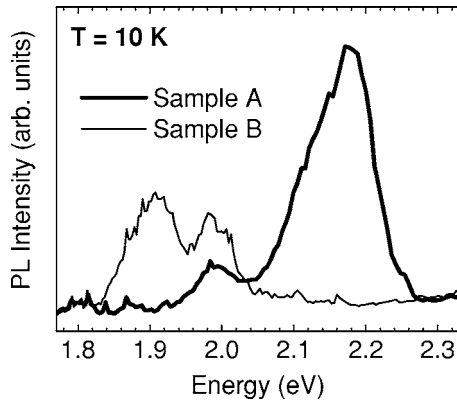


FIG. 5. Micro-PL spectra of InGaP rods from samples A and B. The InGaP rods were transferred to the Si substrate.

metallic spheres (In) at the top of the rods. Figure 4 shows a typical Raman spectrum from a sphere from sample A. The signal intensity is relatively weak compared with the rod signal and it was often smaller than the noise level. From the TO peak position of the measured spectra of spheres from sample A, we estimated an InGaP alloy composition of the order of $\sim 70\%$ of Ga at the spheres, which is in agreement with the Ga composition of the rods. A contribution from the scattered signal coming from the rods may be discarded in those measurements, since the laser was focused at sphere positions relatively far from the rods and the laser probe focus diameter ($\sim 1 \mu\text{m}$) is smaller than the sphere sizes selected for those measurements. This result indicates therefore that the spheres have a small volume composed of an InGaP alloy that was not detected by the microscopic analysis.

A typical Raman spectrum from the substrate surface of sample A, far from any rod, is also shown in Fig. 4. In this case, the spectrum has a marked difference from that observed for the rods and the spheres. Besides the three typical features observed on the InGaP rods, we observe an extra peak at the low-energy side ($\sim 300 \text{ cm}^{-1}$), which is probably due to a vibrational mode of the pure InP substrate. These results indicate the presence of a thin superficial InGaP layer formed on top of the InP substrate. From the TO peak position we estimated that the InGaP layer formed at the surface has an average Ga content of $\sim 70\%$, similar to the material detected at the spheres, which indicates that their formation has a common origin.

We observed that these InGaP microrods present efficient optical emission. For micro-PL measurements, we transferred some InGaP rods from both samples to Si substrates in order to avoid additional emissions from the surface, which also has a thin InGaP alloy layer as discussed above. Before performing the micro-PL measurements, we analyzed the rods on the Si substrate using high-resolution optical microscopy and determined that the rods are well separated from each other, with a distance between them larger than the spot size. Therefore, we discard here the possibility of observing simultaneous emission from more than one rod. The typical micro-PL spectra of the InGaP rods from samples A and B measured at 10 K are shown in Fig. 5. We observe two broadbands with linewidths of $\sim 100 \text{ meV}$.

The higher energy band is associated with excitonic recombinations (free and bound excitons). Using InGaP energy band gap variation as a function of its alloy composition from the literature,¹⁷ we calculated that the PL peak positions correspond to Ga contents of 0.65 and 0.51, for samples A and B, respectively. These results are in good agreement with the composition range estimated by Raman measurements. The relatively broad emission bands must be associated with alloy composition variations along the rods. It is important to mention that the band gap of the InGaP alloy becomes indirect for Ga contents above 0.75. Therefore, the observed luminescence comes only from the rods with Ga composition below this value. The lower energy emission bands correspond to a level ~ 200 and $\sim 100 \text{ meV}$ below the InGaP band-gap energy, for sample A and sample B, respectively. This binding energy is much larger than the binding energies of the usual InGaP impurities such as C and Si, which are of the order of $\sim 50 \text{ meV}$. The peaks associated with those impurities would not be resolved in our experiments. The origin of the low energy bands is likely to be related to defects and vacancies.

IV. DISCUSSION

The presence of the spheres at the top of the rods indicates a growth mechanism similar to that of the VLS growth.⁹ In the case of VLS growth, an extra metal, usually Au nano- or micro-particles, is evaporated onto the sample surface and acts as a growth catalyst. In our samples, however, no extra metal is used. Instead, a substrate component (In) fulfills the role of a microcatalyst. It is known that the congruent InP temperature ($\sim 360 \text{ }^\circ\text{C}$) is smaller than the growth temperature.²⁴ Therefore, under the growth conditions, the InP substrate surface loses P at a rate larger than it loses In. The excess In comes together to form droplets, which has indeed been reported in the case of InP single crystals. Relatively large In droplets have been observed at the sample surface of InP when the sample was heated from 550 up to 750 $^\circ\text{C}$.²⁵ Based on an analogy with the VLS growth mechanism, we offer the following speculations about the growth of our InGaP rods: We expect that when the TMGa flux starts, In droplets are formed at the surface of our samples and they act as growth catalyst areas for the formation of the InGaP rods. The P atoms released from the substrate at the growth temperature plus the Ga atoms supplied by the TMGa flux would then be absorbed by the In droplets, converting them into (In and Ga) alloy clusters. As more Ga and P atoms are absorbed by the (In and Ga) droplets, they will eventually reach a supersaturated state and the growth of the InGaP rods should start by precipitation from the droplet at the liquid-solid interface. However, in order to elucidate the details of the growth mechanism, more investigations are still necessary. The process could qualitatively account for the growth of our scepterlike structures, but it does not predict the alloy composition variations observed in some rods. Recently, Jie *et al.*⁷ described the growth of diameter-modulated ternary oxide Zn_2SnO_4 nanorods via VLS mechanism. They point out to the variations of Zn and (or) Sb vapor concentrations around the alloy droplets as the major

factor for the formation of diameter-modulated nanorods. The composition of an alloy is a parameter sensitive to various growth conditions. One of this is growth temperature, as demonstrated by the decrease in the average Ga composition our rods from 0.7 to 0.5 when the growth temperature was increased from 650 to 700 °C. Additional growth parameters that affect the rod composition are the Ga and P partial pressures, the sphere diameter, i.e., surface tension and contact geometry, and the distance between neighboring rods. Therefore, small variations of these parameters during growth should result in the alloy composition variations observed for some rods. Efforts are now being made to better control these parameters in order to improve the homogeneity of the InGaP free-standing rods.

Another effect that should be considered is spinodal decomposition, where the alloy spontaneously separates in a mixture of phases with different compositions. The critical temperature, above which no spinodal decomposition is expected, is estimated to be around 650 °C for InGaP alloys.^{26–28} Based on these results we should not expect phase decomposition in our structures. However, we cannot rule out this possibility because the spinodal decomposition diagram is rather sensitive to growth details such as strain and diffusion rates of the species at the growth front, parameters that are not well established for the present growth method. Therefore, phase decomposition may occur in our samples especially in the sample grown at 650 °C (sample B). It could also occur in the sample grown at 700 °C (sample A), but in this case, the effect should be weaker. Spinodal decomposition typically results in a redshift of the PL emission, which is dominated by the small band-gap phase.^{29,30} It may also result in a broadening of the emission band and in an additional peak, depending on the sample and the excitation conditions.^{29–31} The low energy band observed for sample B (Fig. 5) could, therefore, be attributed to a smaller band-gap phase (Ga content of ~ 0.48) when compared with the phase associated with the high energy band (Ga content of ~ 0.52). These are reasonable compositions for the spinodal decomposition phases of an alloy with an averaged Ga content of 0.50. It is, however, very unlikely that the low energy band observed for sample A has a similar origin. The energy of the PL bands observed for this sample would correspond to quite different Ga compositions (0.35 and 0.65) and the spinodal decomposition effect should become weaker for sample A, as discussed above. Nonetheless, phase decomposition may be related to the relatively broad emission bandwidth of the high energy band from this sample. The relatively large broadening of the Raman lines is also consistent with the separation of the InGaP alloy in two phases with slightly different compositions, but additional measurements and stronger evidence are still necessary to confirm this.

V. CONCLUSIONS

We investigated InGaP scepterlike structures by optical techniques, comparing the results with microscopic techniques. We demonstrated that Raman scattering is a practical and powerful tool to investigate the properties of self-

sustained rods. It combines the possibility of microscopic measurements from individual structures with the advantages of an easy experimental procedure that may be performed at room temperature. This makes it possible to obtain simultaneously a detailed analysis of a single structure and a large number of measurements from distinct structures for statistical analysis. The Ga content of the InGaP rods shows some variation along their lengths, with a tendency to decrease as the growth temperature is decreased. We observed the presence of long rods, with lengths up to $\sim 30 \mu\text{m}$, with relatively uniform alloy compositions. By Raman-scattering spectroscopy, we detected a small InGaP signal from the surface of the substrate and from the spheres of the rods, indicating that a thin layer of InGaP is also formed in those regions. We also observed an interesting Raman amplification effect around the “neck” (the rod region close to its interface with the sphere) that may be associated with a SERS effect due to the metallic capping layer of the rods. Finally, the InGaP rods have efficient optical emissions, indicating that the InGaP rods grown by this method can be used for optical device applications.

ACKNOWLEDGMENTS

We thank M. M. Tanabe for technical support, F. Cerdeira for useful discussions, and the Brazilian agencies FAPESP, CAPES, and CNPq for financial support.

¹C.-C. Chen and C.-C. Yeh, *Adv. Mater.* (Weinheim, Ger.) **12**, 738 (2000).

²R. Gupta, Q. Xiong, G. D. Mahan, and P. C. Eklund, *Nano Lett.* **3**, 1745 (2003).

³C.-C. Chen *et al.*, *J. Am. Chem. Soc.* **123**, 2791 (2001).

⁴U. Krishnamachari, M. Borgstrom, B. J. Ohlsson, N. Panev, L. Samuelson, W. Seifert, M. W. Larsson, and L. R. Wallenberg, *Appl. Phys. Lett.* **85**, 2077 (2004).

⁵D.-X. Ye, T. Karabacak, B. K. Lim, G.-C. Wang, and T.-M. Lu, *Nanotechnology* **15**, 817 (2004).

⁶R. P. Wang, G. Xu, and P. Jin, *Phys. Rev. B* **69**, 113303 (2004).

⁷J. Jie *et al.*, *J. Phys. Chem. B* **108**, 8249 (2004).

⁸J. Hu, T. W. Odom, and C. M. Lieber, *Acc. Chem. Res.* **32**, 435 (1999).

⁹R. S. Wagner and W. C. Ellis, *Appl. Phys. Lett.* **04**, 89 (1964).

¹⁰W. I. Park, D. H. Kim, S.-W. Jung, and G.-C. Yi, *Appl. Phys. Lett.* **80**, 4232 (2002).

¹¹A. M. Morales and C. M. Lieber, *Science* **279**, 208 (1998).

¹²H.-J. Choi *et al.*, *J. Phys. Chem. B* **107**, 8721 (2003).

¹³M. Sacilotti, J. Decobert, H. Sik, G. Post, C. Dumas, P. Viste, and G. Patriarche, *J. Cryst. Growth* **272**, 198 (2004).

¹⁴M. Gudisken and Ch. Lieber, *J. Am. Chem. Soc.* **122**, 8801 (2000).

¹⁵M. Gudisken, J. Wang, and Ch. Lieber, *J. Phys. Chem. B* **105**, 4062 (2001).

¹⁶T. Kato, T. Matsumoto, and T. Ishida, *Jpn. J. Appl. Phys., Part 1* **27**, 983 (1988).

¹⁷M. Zachau and W. T. Masselink, *Appl. Phys. Lett.* **60**, 2098 (1992).

¹⁸R. Beserman, C. Hirlimann, and M. Balkanski, *Solid State Commun.* **20**, 485 (1976).

¹⁹R. M. Abdelouhab, R. Braunstein, K. Bärner, M. A. Rao, and H. Kroemer, *J. Appl. Phys.* **66**, 787 (1989).

²⁰B. Jusserand and S. Slemkes, *Solid State Commun.* **49**, 95 (1984).

²¹H. Xu, J. Aizpurua, M. Käll, and P. Apell, *Phys. Rev. E* **62**, 4318 (2000).

²²M. Suzuki, Y. Niidome, N. Terasaki, K. Inoue, Y. Kuwahara, and S. Yamada, *Jpn. J. Appl. Phys., Part 2* **43**, 554 (2004).

²³G. D. Mahan, R. Gupta, Q. Xiong, C. K. Adu, and P. C. Eklund, *Phys. Rev. B* **68**, 073402 (2003).

²⁴B. E. Gordon, A. S. W. Lee, D. A. Thompson, and B. J. Robinson, *Semicond. Sci. Technol.* **18**, 782 (2003).

²⁵M. Sacilotti, R. A. Masut, and A. P. Roth, *Appl. Phys. Lett.* **48**, 481 (1986).

²⁶V. G. Deibuk, *Semiconductors* **37**, 1151 (2003).

- ²⁷O. Schuler, X. Wallart, and F. Mollot, *J. Cryst. Growth* **201**, 280 (1999).
- ²⁸S.-H. Wei, L. G. Ferreira, and A. Zunger, *Phys. Rev. B* **41**, 8240 (1990).
- ²⁹L. S. Vavilova *et al.*, *Semiconductors* **32**, 590 (1998).
- ³⁰R. T. Lee, C. M. Fetzer, S. W. Jun, D. C. Chapman, J. K. Shurtleff, G. B. Stringfellow, Y. W. Ok, and T. Y. Seong, *J. Cryst. Growth* **233**, 490 (2001).
- ³¹A. A. Bernussi, W. Carvalho, Jr., and M. K. K. D. Franco, *J. Appl. Phys.* **89**, 4898 (2001).